Supporting Information

Programmed Delivery of Cyclopeptide RA-V and Antisense Oligonucleotide for Combination Therapy on Hypoxic Tumors and Therapeutic Self-Monitoring

Yongrong Yao,‡ Li Feng,‡ Zhe Wang, Huachao Chen,* Ninghua Tan*

State Key Laboratory of Natural Medicines, Jiangsu Key Laboratory of TCM Evaluation and Translational Research, School of Traditional Chinese Pharmacy, China Pharmaceutical University, Nanjing 211198, China.

*Corresponding author, Ninghua Tan, Email: nhtan@cpu.edu.cn；huachao.chen@163.com

‡These authors contributed equally

Additional Figures

1. Fig. S1. TEM micrographs of the RA/RX Liposome at pH 5.0, 6.0 and 7.4.

2. Fig. S2. Size distribution of the nanoparticle characterized by Malvern Instruments at 25 °C.

3. Fig. S3. Zeta distribution of the RA/RX Liposome (without anti-DR5 modification) compared with RA/RX Liposome (-29.83 ± 0.75 mV), characterized by Malvern Instruments at 25 °C.

4. Fig. S4. Zeta distribution of the RA/RX Liposome compared with RA/RX Liposome (without anti-DR5 modification) (-44.2 ± 0.1 mV), characterized by Malvern Instruments at 25 °C.

5. Fig. S5. In vitro release profiles of RX-0047 from the RA/RX Liposome at pH 5.0, 6.0 and 7.4.

6. Fig. S6. In vitro release profiles of the caspase 8 probe from the RA/RX Liposome at pH 5.0, 6.0 and 7.4.

7. Fig. S7. Quantitative fluorescent intensities data of HCT116 cells fluorescence images in Fig. 3a.

8. Fig. S8. Colocalization images of the RX-0047 Liposome in HCT116 cells.

9. Fig. S9. Colocalization images of the RA/RX Liposome (non-DR5) in HCT116 cells.

10. Fig. S10. Confocal fluorescence images of apoptosis by the JC-1 assay in HCT116 and HT29 cells treated with the RA/RX Liposome for 0 h or 12 h.

11. Fig. S11. The blots in Fig.5d were analyzed by optical densitometry using Image J.

12. Fig. S12. The levels of HIF-1α protein in cells upon treatments with different concentrations of the RX-0047 Liposome were also investigated, which were tested in the total cell lysates from HCT 116 cells.

13. Fig. S13. Confocal fluorescence images showing increased intracellular O_2 level after treated with the RA/RX Liposome.

14. Fig. S14. Tumor weights of different groups of HCT116 cells tumor-bearing nude mice after various administrations.

15. Fig. S15. Changes of relative tumor volume upon treatments with different concentrations of the RA/RX Liposome on HCT116 cells tumor-bearing nude mice.

16. Fig. S16. H&E stained images of major organs for in vivo toxicity assay. Histological observation of the organs collected from HCT116 cells tumor-bearing nude mice after different treatments.

17. Fig. S17. The evaluation of levels of serum ALT, AST, creatinine and BUN in different groups after various administrations.

18. Fig. S18. Fluorescence images of activities of caspase-8 in HCT116 tumor-bearing mice with i.v. injection of caspase 8 probe Liposome, RX-0047 Liposome, RA-V Liposome and RA/RX Liposome recorded at 12 h.

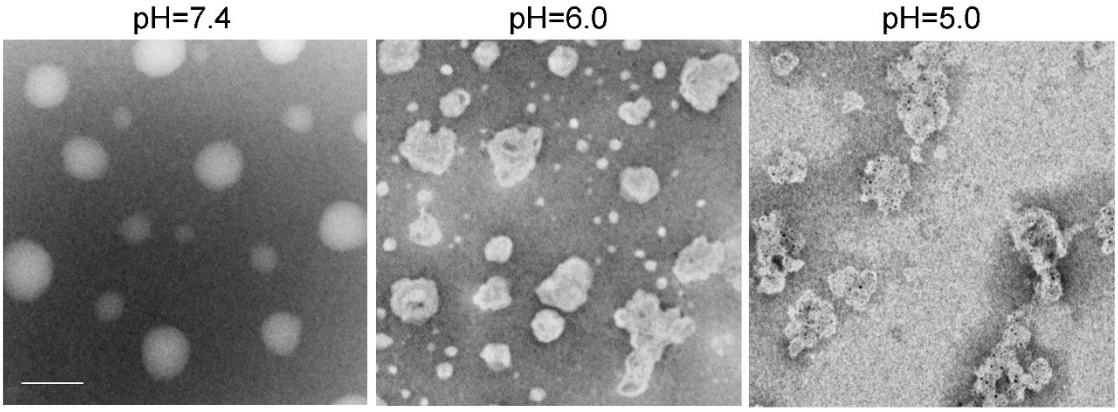

Fig. S1. TEM micrographs of the RA/RX Liposome at pH 5.0, 6.0 and 7.4. Scale bar: 200 nm.

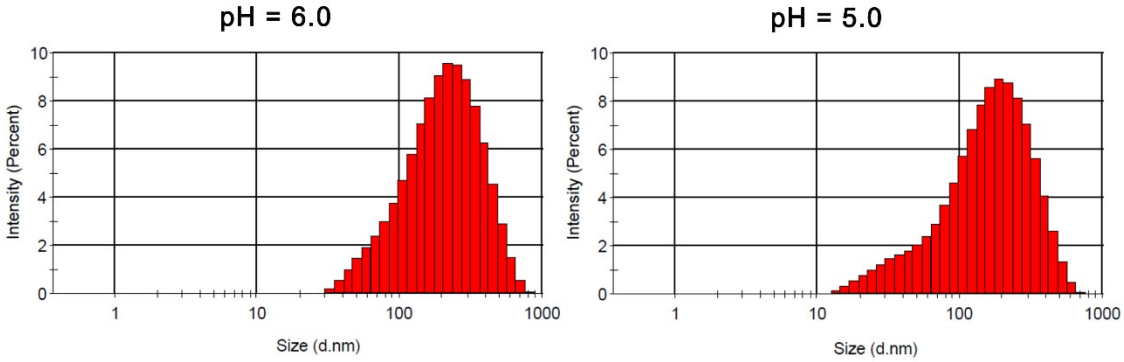

Fig. S2. Size distribution of the nanoparticle characterized by Malvern Instruments at 25 °C. (pH = 6.0: 151 ± 2.21 nm; pH = 5.0: 111.07 ± 2.35 nm)

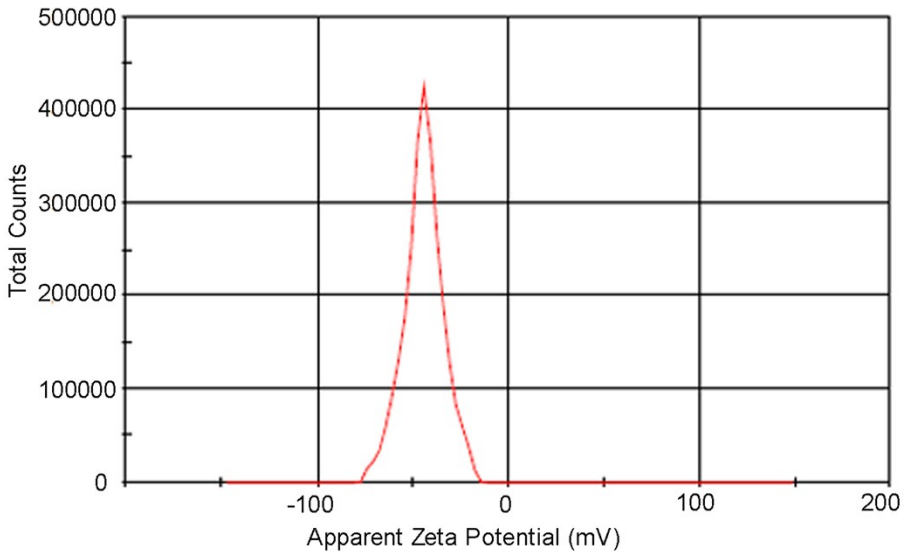

Fig. S3. Zeta distribution of the RA/RX Liposome (without anti-DR5 modification) were -44.2 ± 0.1 mV, compared with the RA/RX Liposome (-29.83 ± 0.75 mV), characterized by Malvern Instruments at 25 °C.

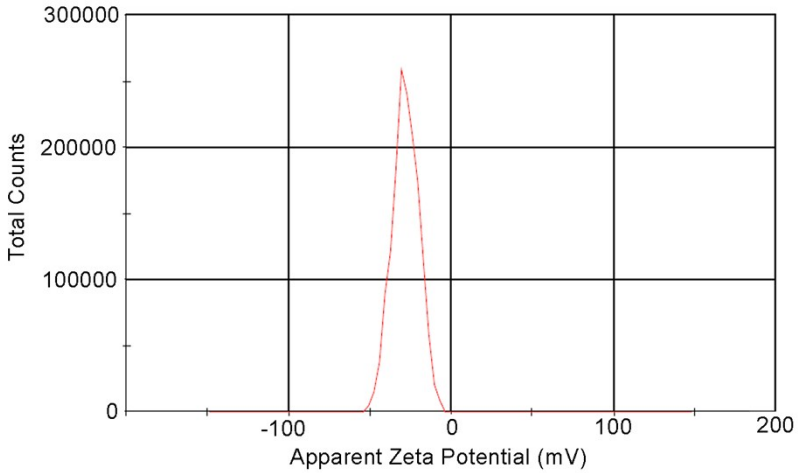

Fig. S4. Zeta distribution of the RA/RX Liposome were -29.83 ± 0.75 mV, compared with the RA/RX Liposome (without anti-DR5 modification) (-44.2 ± 0.1 mV), characterized by Malvern Instruments at 25 °C.

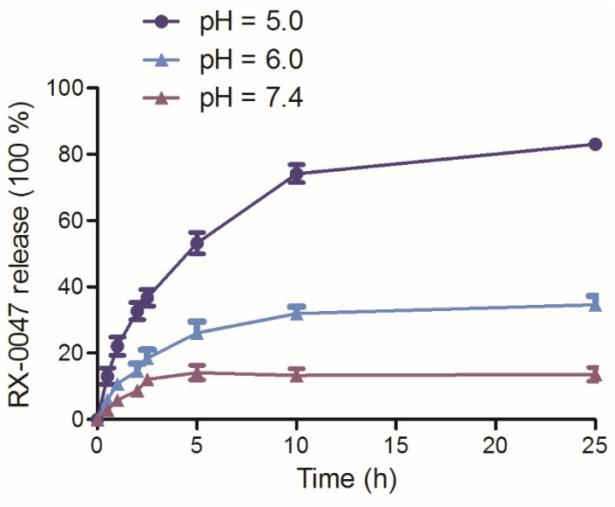

Fig. S5. In vitro release profiles of RX-0047 from the RA/RX Liposome at pH 5.0, 6.0 and 7.4. Data are given as mean ± SD (n = 3).

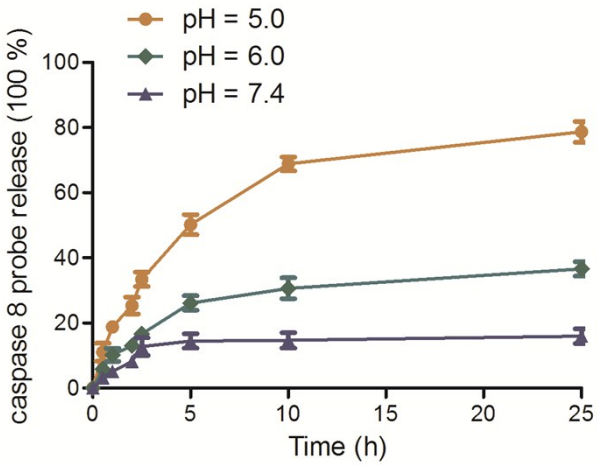

Fig. S6. In vitro release profiles of the caspase 8 probe from the RA/RX Liposome at pH 5.0, 6.0 and 7.4. Data are given as mean ± SD (n = 3).

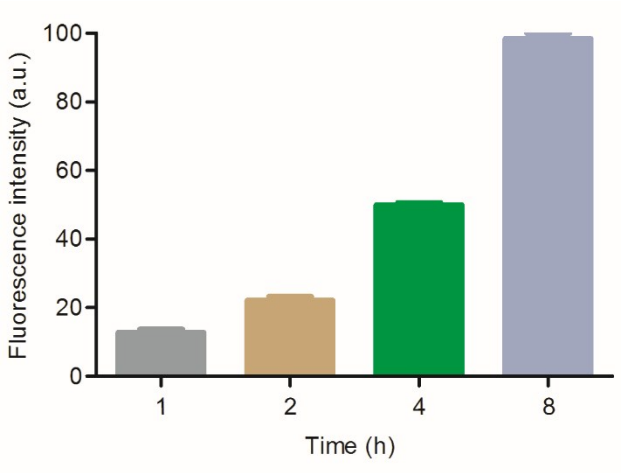

Fig. S7. Quantitative fluorescent intensities data of HCT116 cells fluorescence images in Fig. 3a. Data are given as mean ± SD (n = 3).

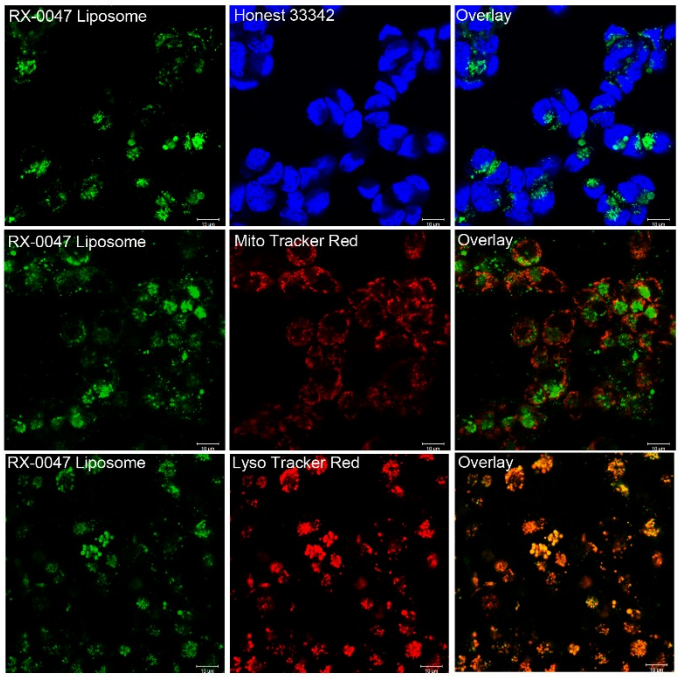

Fig. S8. Colocalization images of the RX-0047 Liposome in HCT116 cells. Cells were incubated with the RX-0047 Liposome for 3 h and then incubated with 100 nM Hoechst 33342, MitoTracker Red, or LysoTracker Red for 10 minutes. Scale bars: 10 μm.

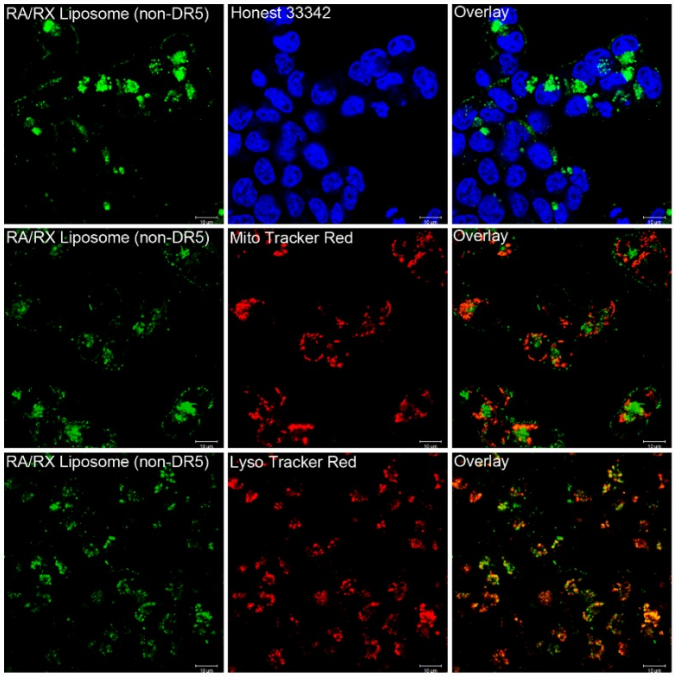

Fig. S9. Colocalization images of the RA/RX Liposome (non-DR5) in HCT116 cells. Cells were incubated with the RA/RX Liposome (non-DR5) for 3 h and then incubated with 100 nM Hoechst 33342, MitoTracker Red, or LysoTracker Red for 10 minutes. Scale bars: 10 µm.

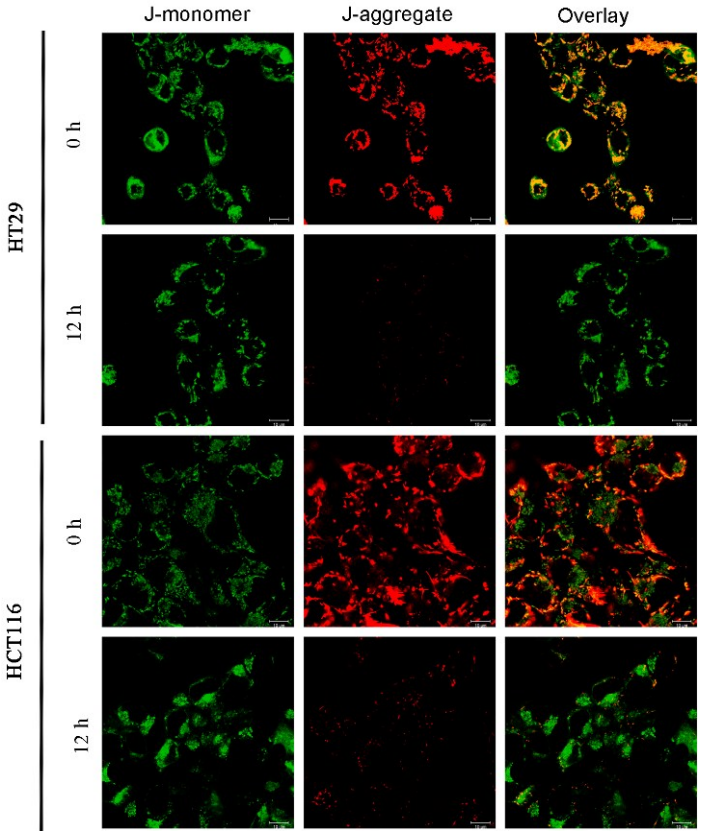

Fig. S10. Confocal fluorescence images of apoptosis by the JC-1 assay in HCT116 and HT29 cells treated with the RA/RX Liposome for 0 h or 12 h. Scale bars: 10 µm.

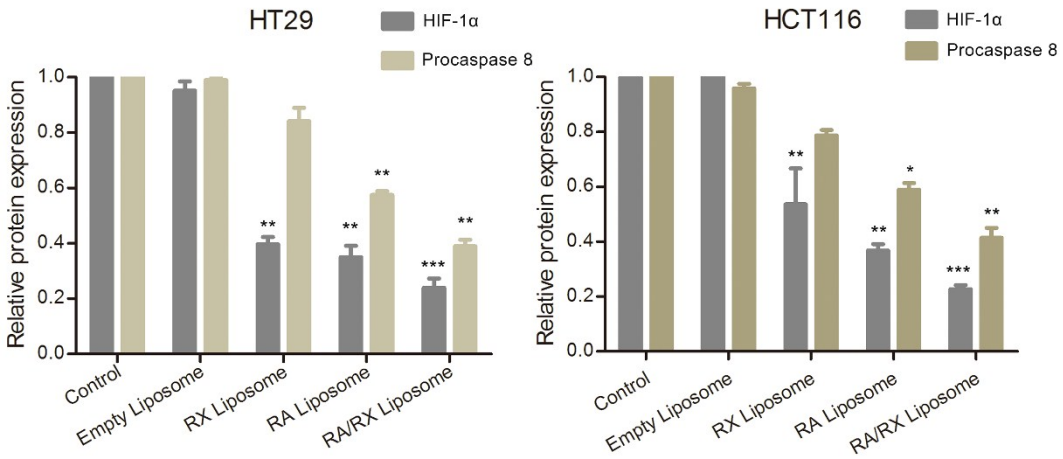

Fig. S11. The blots in Fig. 5d were analyzed by optical densitometry using Image J. Data are expressed as mean ± SD. *$P < 0.05$, **$P < 0.01$, ***$P < 0.001$, compared with control group.

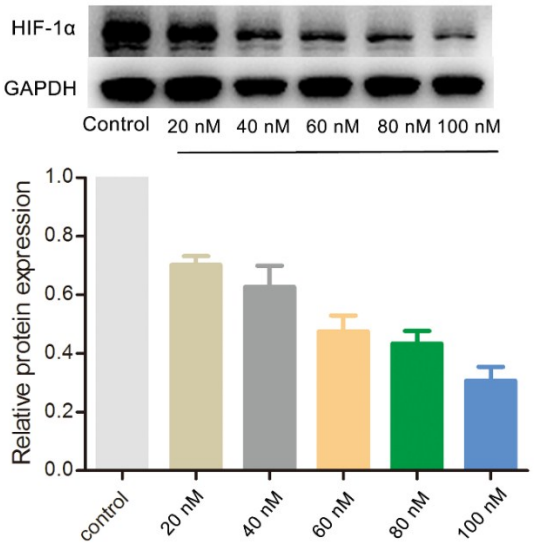

Fig. S12. The levels of HIF-1α protein in cells upon treatments with different concentrations of the RX-0047 Liposome were also investigated, which were tested in the total cell lysates from HCT 116 cells.

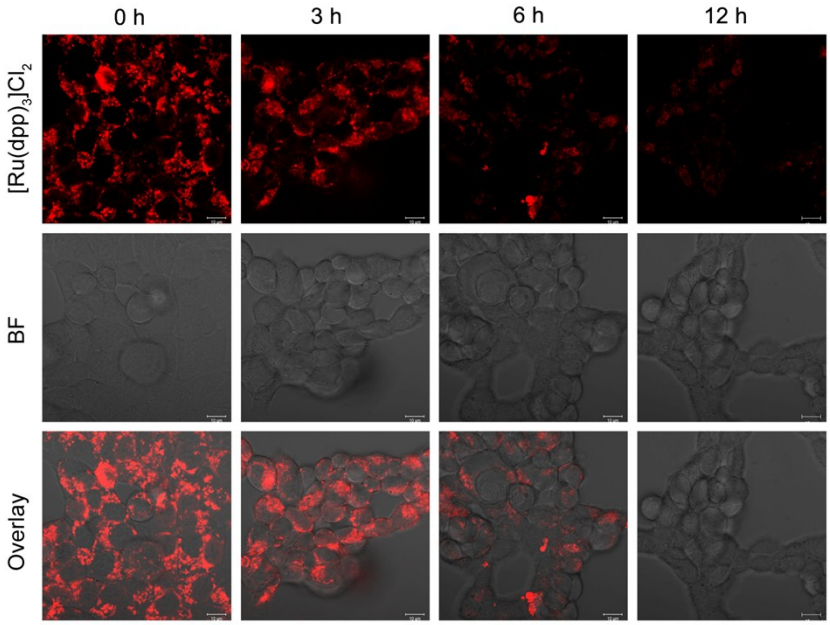

Fig. S13. Confocal fluorescence images showing increased intracellular O_2 level after treated with the RA/RX Liposome. HCT116 cells were incubated with 5 μM $[Ru(dpp)_3]Cl_2$ for 4 h, followed by incubation with the RA/RX Liposome for 0 h, 3 h, 6 h, 12 h. Scale bars: 10 μm.

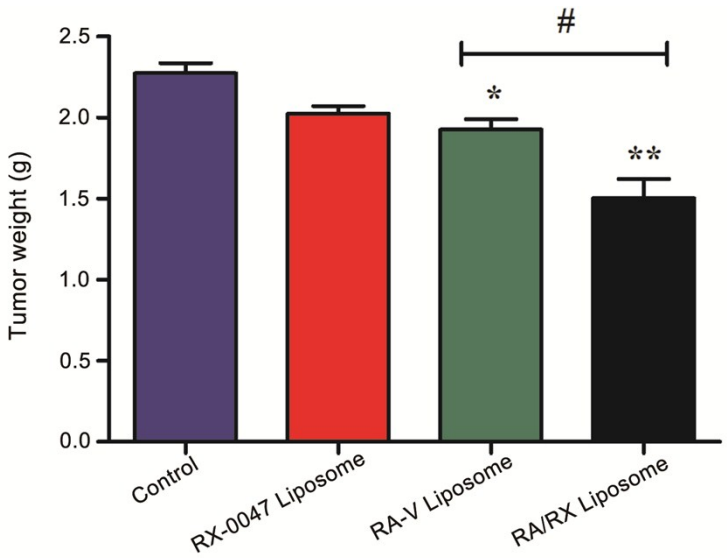

Fig. S14. Tumor weights of different groups of HCT116 cells tumor-bearing nude mice after various administrations. $^{*}P < 0.05$, $^{**}P < 0.01$, $^{\#}P < 0.05$.

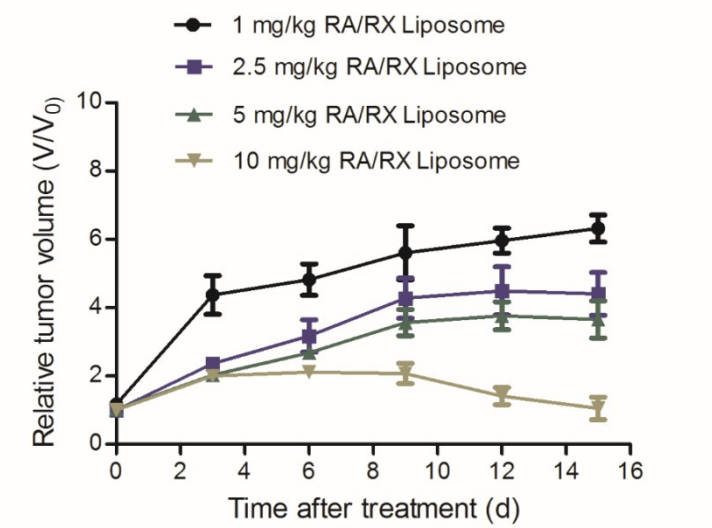

Fig. S15. Changes of relative tumor volume upon treatments with different concentrations of the RA/RX Liposome on HCT116 cells tumor-bearing nude mice.

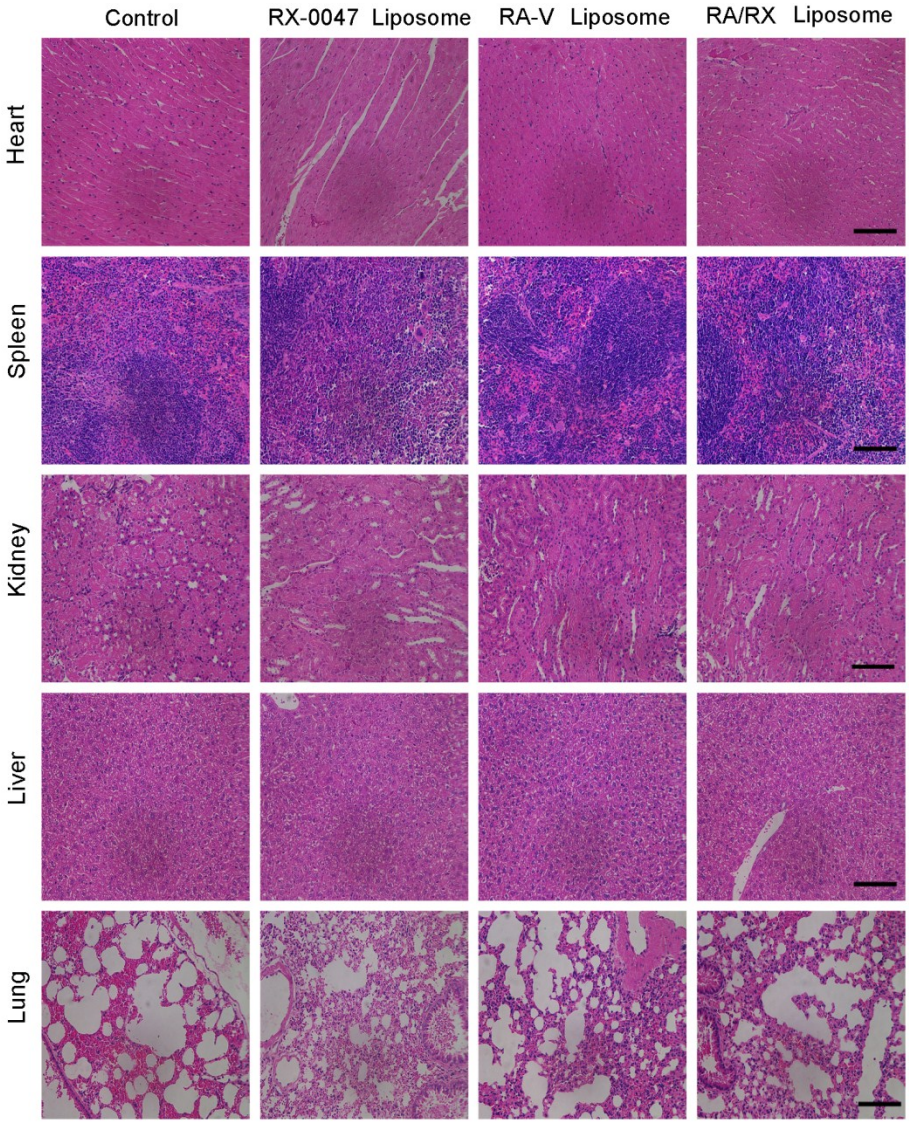

Fig. S16. H&E stained images of major organs for in vivo toxicity assay. Histological observation of the organs collected from HCT116 cells tumor-bearing nude mice after different treatments. No obvious organ damages were observed in major organs. Scale bars: 100 μm.

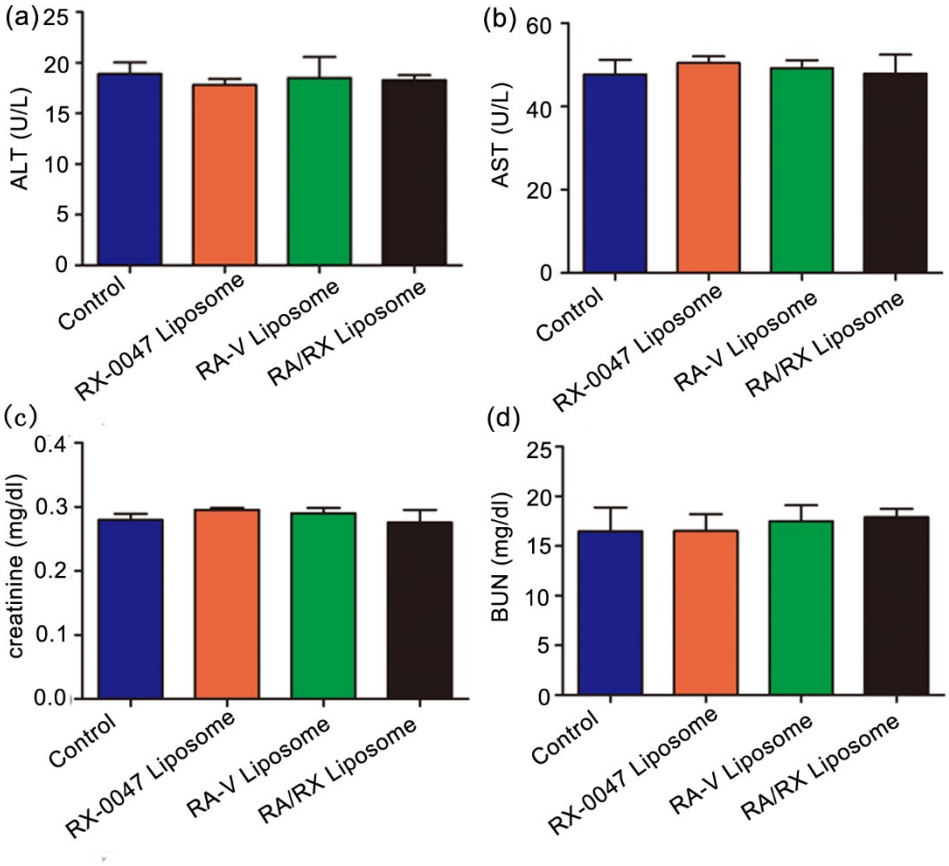

Fig. S17. The evaluation of levels of serum ALT, AST, creatinine and BUN in different groups after various administrations.

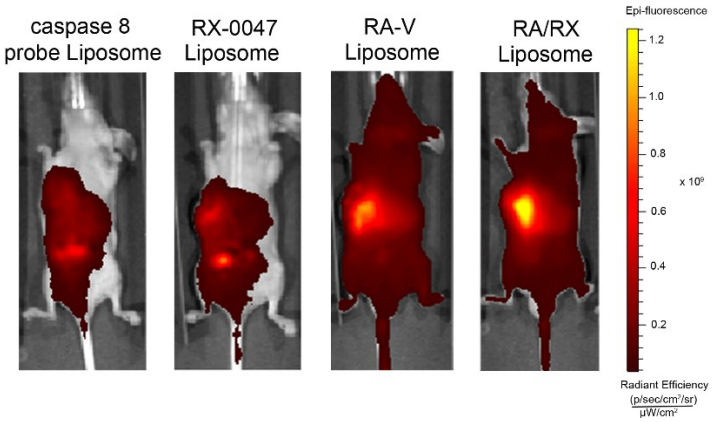

Fig. S18. Fluorescence images of activities of caspase-8 in HCT116 tumor-bearing nude mice with i.v. injection of caspase 8 probe Liposome, RX-0047 Liposome, RA-V Liposome and RA/RX Liposome recorded at 12 h.